



Measurement of the $p\bar{p} \rightarrow WZ + X$ cross section at $\sqrt{s} = 1.96$ TeV and limits on WWZ trilinear gauge couplings

J. D. Degenhardt, A. Alton, A. Askew, H. T. Diehl, B. Zhou
(Dated: August 7, 2007)

We present measurements of the process $p\bar{p} \rightarrow WZ + X \rightarrow \ell'\nu_{\ell'}\ell\bar{\ell}$ at $\sqrt{s} = 1.96$ TeV, where ℓ and ℓ' are electrons or muons. Using 1 fb^{-1} of data from the D0 experiment, we observe 13 candidates with an expected background of 4.5 ± 0.6 events. We measure a cross section $\sigma_{WZ} = 2.7_{-1.3}^{+1.7}$ pb. Using the Z boson transverse momentum distribution, limits on the trilinear WWZ gauge couplings are determined to be $-0.17 \leq \lambda_Z \leq 0.21$ ($\Delta\kappa_Z = 0$) at the 95% C.L. and for form factor scale $\Lambda = 2$ TeV. Further, assuming that $\Delta g_1^Z = \Delta\kappa_Z$, we find $-0.12 \leq \Delta\kappa_Z \leq 0.29$ ($\lambda_Z = 0$) at the 95% C.L. These are the most restrictive limits on the WWZ couplings available.

The $SU(2)_L \times U(1)_Y$ structure of the standard model (SM) Lagrangian requires that the massive electroweak gauge bosons, the W and Z bosons, interact with one another through trilinear and quadrilinear vertices. In the SM, the production cross section for $p\bar{p} \rightarrow WZ + X$ ($\sigma(WZ)$) depends on the strength of the WWZ coupling, which is $-e \cot \theta_W$, where e is the positron charge and θ_W is the weak mixing angle. At $\sqrt{s} = 1.96$ TeV, the SM predicts $\sigma_{WZ} = 3.68 \pm 0.25$ pb [1]. Any significant deviation from this prediction would be evidence for new physics.

Excursions of the WWZ interactions from the SM prediction can be parameterized by a generalized effective Lagrangian [2, 3]

$$\frac{\mathcal{L}_{WWZ}}{g_{WWZ}} = ig_1^Z (W_{\mu\nu}^\dagger W^\mu Z^\nu - W_\mu^\dagger Z_\nu W^{\mu\nu}) + i\kappa_Z W_\mu^\dagger W_\nu Z^{\mu\nu} + i\frac{\lambda_Z}{M_W^2} W_{\rho\mu}^\dagger W^\mu{}_\nu Z^{\nu\rho}$$

with $g_{WWZ} = -e \cot \theta_W$ and trilinear gauge couplings (TGCs) g_1^Z , κ_Z , and λ_Z describing the coupling strengths of the vector bosons to the weak field. These excursions are manifestations of new physics that result in an enhancement in the production cross section as well as modifications to the shapes of kinematic distributions, such as the Z boson transverse momentum $p_T(Z)$. The TGC parameters are commonly measured as deviations from their SM values, or as $\Delta g_1^Z = |g_1^Z - 1|$, $\Delta\kappa_Z = |\kappa_Z - 1|$, and λ_Z , where $\lambda_Z = 0$ in the SM. Because the Fermilab Tevatron is the first particle accelerator that can produce the charged state $WZ + X$, this measurement provides a unique opportunity to study the WWZ TGCs without any assumption on the values of the $WW\gamma$ couplings.

WZ production measurements and studies of WWZ couplings have been presented previously. The D0 Collaboration measured $\sigma_{WZ} = 4.5_{-2.6}^{+3.8}$ pb, with a 95% C.L. upper limit of 13.3 pb, using 0.3 fb^{-1} of $p\bar{p}$ collisions at $\sqrt{s} = 1.96$ TeV [4]. The observed number of candidates was used to form the tightest available limits on anomalous WWZ couplings. More recently, the CDF Collaboration found $\sigma_{WZ} = 5.0_{-1.6}^{+1.8}$ pb using 1.1 fb^{-1} of $p\bar{p}$ collisions at $\sqrt{s} = 1.96$ TeV [5], but did not present any results on WWZ couplings.

This paper describes a significant improvement to the previous D0 analysis. Not only is the data sample more than three times larger, but an improved technique is used to constrain the WWZ couplings. Namely, the p_T distribution of the Z bosons, instead of merely the total number of events, produced in the collisions are compared against the expectations of non-SM WWZ couplings. Use of the kinematic variable $p_T(Z)$ significantly increases the power of the WWZ coupling measurement over previous measurements [4, 6], which used only the number of events observed.

We search for WZ candidate events in three charged lepton final states, referred to as trileptons, produced when $Z \rightarrow \ell^+\ell^-$ and $W \rightarrow \ell'\nu$, where ℓ and ℓ' are e^\pm or μ^\pm . SM backgrounds can be suppressed by requiring three isolated high p_T leptons and large missing transverse energy (\cancel{E}_T) from the neutrino. However, limiting the signal to trilepton decay modes reduces the combined branching fraction for the four possible final states (eee , $ee\mu$, $\mu\mu e$ and $\mu\mu\mu$) to 1.5% [7].

The D0 detector is a multipurpose detector that collects $p\bar{p}$ collisions at the Fermilab Tevatron. D0 is composed of several subdetectors and a fast electronics triggering system which is described in detail in Ref. [8]. At the center of

the detector is a central tracking system, consisting of a silicon microstrip tracker (SMT) and a central fiber tracker (CFT), both located within a 2 T superconducting solenoidal magnet. These detectors have designs optimized for tracking and vertexing at pseudorapidities [9] $|\eta| < 3$ and $|\eta| < 2.5$, respectively. The liquid-argon and uranium calorimeter has a central section (CC) covering $|\eta| < 1.1$, and two end calorimeters (EC) that extend coverage to $|\eta| \approx 4.2$, with all three housed in separate cryostats [10]. An outer muon system, at $|\eta| < 2$, consists of a layer of tracking detectors and scintillation trigger counters in front of 1.8 T toroids, followed by two similar layers after the toroids [11].

Electrons are identified by their distinctive pattern of energy deposition in the calorimeter and by the presence of a track in the central tracker that can be extrapolated from the interaction vertex to a cluster of energy in the calorimeter. Electrons measured in the CC (EC) must have $|\eta| < 1.1$ ($1.5 < |\eta| < 2.5$). The transverse energy of an electron must satisfy $E_T > 15$ GeV and it must be isolated from other energy clusters. A likelihood variable, formed from the quality of the electron track and its spatial and momentum match to the calorimeter cluster and the calorimeter cluster information, is used to discriminate electron candidates from instrumental backgrounds.

Muons are reconstructed using information from the muon draft chambers and scintillation detectors, central tracking detectors, and the calorimeters. A muon reconstructed in the muon detectors must have a matching central track with $p_T > 15$ GeV/ c . Candidate muons are required to be isolated in the calorimeter and tracker to minimize the contribution of muons originating from jets. More detail is available in [12].

Candidate events were collected with single muon and single electron and di-electron triggers. The analysis starts with events that have reconstructed dileptons (jets) collected from 2002–2006 for signal (background) studies. The integrated luminosities [13] for the eee , $ee\mu$, $\mu\mu e$, and $\mu\mu\mu$ final states are 1070 pb $^{-1}$, 1020 pb $^{-1}$, 944 pb $^{-1}$, and 944 pb $^{-1}$, respectively. There is a common 6.1% uncertainty on the integrated luminosities.

The WZ event selection requires three reconstructed, well-isolated leptons with $p_T > 15$ GeV/ c . All three leptons must be associated with isolated tracks that originate from the same collision point and must pass the electron or muon identification criteria outlined above. To select Z bosons, and further suppress background, the invariant mass of a like-flavor lepton pair must fall within the range 71 to 111 GeV/ c^2 for $Z \rightarrow ee$ events, and 50 to 130 GeV/ c^2 for $Z \rightarrow \mu\mu$ events, with the mass windows set by the mass resolution. For eee and $\mu\mu\mu$ decay channels, the lepton pair with invariant mass closest to that of the Z boson mass are chosen as the Z boson daughter particles. The \cancel{E}_T is required to be greater than 20 GeV, consistent with the decay of a W boson. The transverse recoil of the WZ system, calculated using the vector sum of the transverse momenta of the charged leptons and missing transverse energy, is required to be less than 50/ c GeV. This selection reduces the background contribution from $t\bar{t}$ production to a negligible level.

Kinematic and geometric acceptances range from 29% for the eee decay mode to 45% for the $\mu\mu\mu$ decay mode. It is also necessary to account for τ final states of WZ production that subsequently decay leptonically thereby contributing to the signal. The number of τ events expected to pass the event selection is 0.67 ± 0.11 events. These are treated as signal in the cross section analysis.

WZ event detection efficiencies are determined for each of the four decay modes from Monte Carlo (MC) simulation and from studies of Z bosons in D0 data. The average efficiencies for detecting an electron or muon with E_T (p_T) > 15 GeV are $(91 \pm 2)\%$ and $(90 \pm 2)\%$, respectively. The trigger efficiency for events with two (or more) electrons is estimated to be $(99 \pm 1)\%$. For events with two or three muons, the trigger efficiencies are estimated to be $(91 \pm 5)\%$ and $(98 \pm 2)\%$, respectively. Table I summarizes the efficiency determinations for the four decay modes.

A total of 13 WZ candidate events is found. Figure 1 shows the \cancel{E}_T versus the dilepton invariant mass for the background, the expected number of WZ events, and the data, including the candidates. Table 1 details the number of candidates in each channel.

The main backgrounds for $WZ \rightarrow \ell'\nu\ell\ell$ are $Z + X$ events where X is either a jet or photon that has been misidentified as an electron or muon. We assess backgrounds from Z +jets production by using a large inclusive jet data sample that is selected with an independent jet trigger. Events characteristic of QCD two-jet production are used to measure the probability, as a function of jet E_T and η , that a single jet will be misidentified as a muon or electron. Next, sub-samples of ee +jets, $e\mu$ +jets, and $\mu\mu$ +jets events are selected from the inclusive jet sample using the same criteria as for the WZ signal except that the requirements for a third lepton in the event are dropped. The single jet-lepton misidentification probabilities are then convoluted with the measured jet distributions in the dilepton+jets sub-samples to provide an estimate of the background from Z +jets events. The summed contribution for all four decay modes is 1.3 ± 0.1 events.

All other backgrounds are determined using MC methods which typically entail a set of events generated using the PYTHIA event generator [14]. The events are subsequently processed through a detector simulation [15] and the same reconstruction chain as was used for the data. Non-negligible backgrounds include SM ZZ production, $Z\gamma$ production, and W^*Z , WZ^* , or $W\gamma^*$ (“Drell-Yan”) production. We define Drell-Yan processes as three-lepton final states produced through the decay of one on-mass-shell and one off-shell vector boson. These backgrounds and their determination are described as follows.

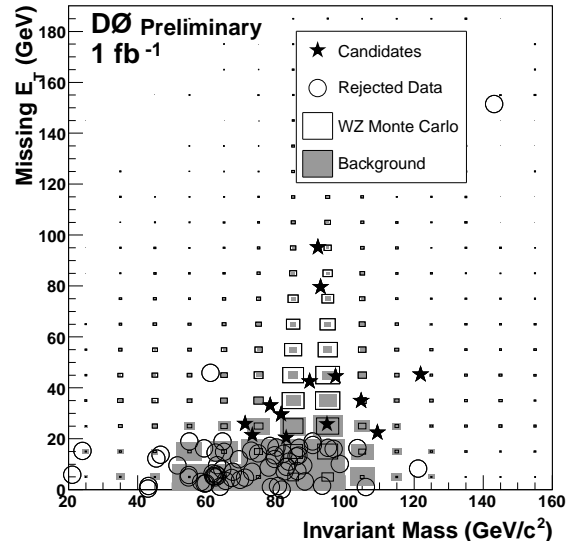


FIG. 1: \cancel{E}_T versus dilepton invariant mass of WZ candidate events. The open boxes correspond to the signal expectation. The grey boxes correspond to the sum of the estimated backgrounds. The black stars are the data that survive all selection criteria. The open circles are data that fail either the dilepton invariant mass criterion or have $\cancel{E}_T < 20$ GeV.

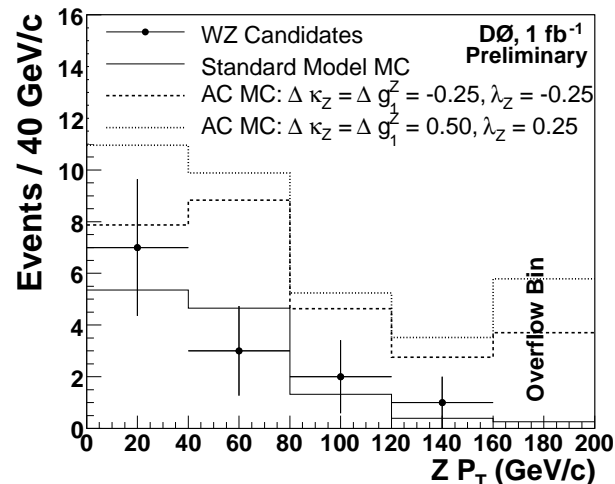


FIG. 2: The reconstructed Z boson p_T of the WZ candidate events used in the WWZ coupling parameter limit setting procedure. The solid histogram is the expected sum of signal and background for the case of the WWZ coupling parameters set to their SM values. The dotted and double dotted histograms are the expected sums of signal and background for two different cases of anomalous WWZ coupling parameter values. The black dots are the observed data. The final bin is the overflow bin.

ZZ production becomes a background when both Z bosons decay to charged leptons and one of the final state leptons escapes detection, thus mimicking a neutrino. The total contribution from ZZ production is estimated to be 0.70 ± 0.08 events.

$Z\gamma$ final states can be mis-reconstructed as WZ events if the photon is misidentified as an electron; this affects only the eee and $\mu\mu e$ modes. Here a photon converts to an e^+e^- pair or randomly matches a track in the detector causing it to be mis-identified as an electron. We estimate the $\ell\bar{\ell} + \gamma$ contribution using the Baur MC [16] folded with the probability for a photon to be misidentified as an electron determined from a PYTHIA plus GEANT MC of $Z + \gamma \rightarrow \ell\bar{\ell}\gamma$ final state radiation events. By examining the sample of these events where the three body mass falls within the Z mass window, we can use these events as a pure sample of photons from which an efficiency of photons

TABLE I: The numbers of candidate events, expected signal events, and estimated background events, and the overall detection efficiency for the four final states.

Final State	Number of Candidate Events	Expected Signal Events	Estimated Background Events	Overall Efficiency
eee	2	2.3 ± 0.2	1.2 ± 0.1	0.16 ± 0.02
$ee\mu$	1	2.2 ± 0.2	0.46 ± 0.03	0.17 ± 0.02
$\mu\mu e$	8	2.2 ± 0.3	2.0 ± 0.4	0.17 ± 0.03
$\mu\mu\mu$	2	2.5 ± 0.4	0.86 ± 0.06	0.21 ± 0.03
Total	13	9.2 ± 1.0	4.5 ± 0.6	–

TABLE II: One-dimensional 95% C.L. intervals on λ_Z , Δg_1^Z , and $\Delta\kappa_Z$ for two sets of the cut off value, Λ .

$\Lambda = 1.5$ TeV	$\Lambda = 2.0$ TeV
$-0.18 < \lambda_Z < 0.22$	$-0.17 < \lambda_Z < 0.21$
$-0.15 < \Delta g_1^Z < 0.35$	$-0.14 < \Delta g_1^Z < 0.34$
$-0.14 < \Delta\kappa_Z = \Delta g_1^Z < 0.31$	$-0.12 < \Delta\kappa_Z = \Delta g_1^Z < 0.29$

to pass the electron cuts is determined. This efficiency is folded with MC $\ell\bar{\ell} + \gamma$ events to determine this background contribution. The contribution from this background is estimated to be 1.4 ± 0.5 events.

It is important to also account for the Drell-Yan continuum when measuring the cross-section for WZ production, where the Z boson is considered to be on-shell. This contribution is not accounted for in the signal MC, nor in the cross section prediction, and is treated as background. The amount of Drell-Yan that is estimated to be in our signal is 0.99 ± 0.19 events. This is determined by comparing PYTHIA-generated Drell-Yan events in the signal region to PYTHIA-generated on-shell Z bosons and scaling that ratio to the expected number of WZ candidates in each channel.

To cross check the background estimates, we compare the number of observed events with that expected when we do not apply the dilepton invariant mass selection and the \cancel{E}_T selection. We expected to see 12.5 ± 1.4 events from signal and 62.9 ± 8.4 events from all of the backgrounds, and we observe 78 events. This agreement is also reflected in Fig. 1.

The SM predicts that 9.2 ± 1.0 events are expected to be observed in the data sample. The probability for the background, 4.5 ± 0.6 events, to fluctuate to 13 or more events is 1.2×10^{-3} , which translates to a one-sided Gaussian significance of 3.0σ . This probability is determined by using a Gaussian probability to model the background uncertainty which is then convoluted with a Poissonian fluctuation probability. A likelihood method is used to determine the most likely cross section. The likelihood is determined as a function of cross section in each channel. The log likelihoods are then combined and the minimum of the negative log likelihood determines the most likely cross section [17]. The cross section for WZ production is measured to be $2.7_{-1.3}^{+1.7}$ pb, where the $\pm 1\sigma$ errors are the 68% C.L. limits from the minimum of the negative log likelihood.

By comparing the measured cross section and $p_T(Z)$ distribution to models with anomalous TGCs, we set one- and two-dimensional limits on the three CP -conserving coupling parameters. A comparison of the observed Z boson p_T distribution with MC predictions is shown in Fig. 2. We use the Hagiwara-Woodside-Zeppenfeld (HWZ) [18] leading order event generator processed with a fast detector and event reconstruction simulation to produce events with anomalous WWZ couplings and simulate their efficiencies and acceptances. The HWZ event generator does not account for tau lepton final states, and as a result, we treat the estimated tau contribution, 0.7 events, as background for the WWZ coupling limit setting procedure. The method used to determine the coupling limits is described in Ref. [19]. Limits are set on the coupling parameters λ_Z , Δg_1^Z ($\equiv g_1^Z - 1$), and $\Delta\kappa_Z$. Two-dimensional grids are constructed in which the parameters λ_Z and Δg_1^Z are allowed to vary simultaneously. Table II presents the one-dimensional 95% C.L. limits on λ_Z , Δg_1^Z and $\Delta\kappa_Z$. Figure 3 presents the two-dimensional 95% C.L. limits under the assumption $\Delta g_1^Z = \Delta\kappa_Z$ [3] for $\Lambda = 2$ TeV. Figure 4 presents the two-dimensional 95% C.L. limits in λ_Z versus Δg_1^Z with $\Delta\kappa_Z = 0$ for $\Lambda = 2$ TeV. The form factor, Λ [20], associated with each grid is chosen such that the limits are within the unitarity bound.

The D0 Collaboration has searched for WZ production in 1.0 fb^{-1} of $p\bar{p}$ collisions at $\sqrt{s} = 1.96$ TeV. We measure the WZ production cross section to be $2.7_{-1.3}^{+1.7}$ pb. We observe 13 trilepton candidate events with an expected 9.2 ± 1.0 signal events and 4.5 ± 0.6 events coming from background. This gives a significance of 3.0σ . We use the measured cross section and $p_T(Z)$ distribution to improve constraints on WWZ trilinear gauge couplings by a factor of two

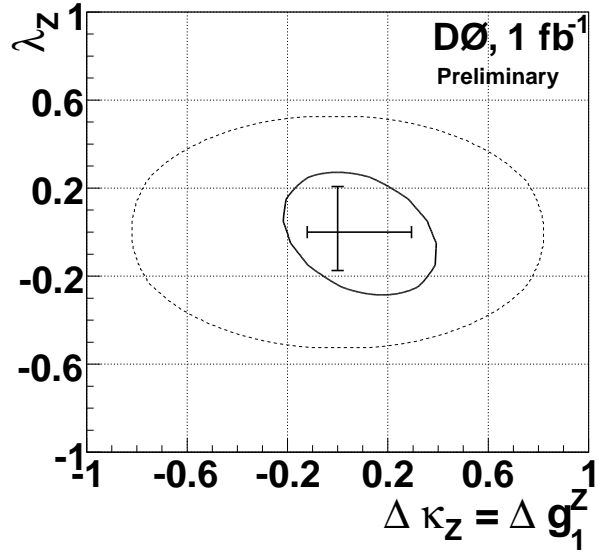


FIG. 3: Two-dimensional 95% C.L. contour limit in $\Delta g_1^Z = \Delta \kappa_Z$ versus $\Delta \lambda_Z$ space (inner contour). The energy scale cut off limit for this contour is $\Lambda = 2$ TeV. The physically allowed region (unitarity limit) is bounded by the outer contour. The cross hairs are the 95% C.L. one-dimensional limits.

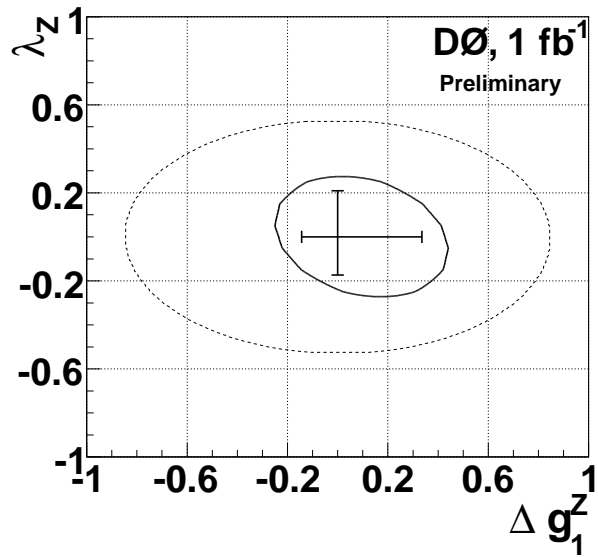


FIG. 4: Two-dimensional 95% C.L. contour limit in Δg_1^Z versus $\Delta \lambda_Z$ space (inner contour) with $\Delta \kappa_Z = 0$. The energy scale cut off limit for this contour is $\Lambda = 2$ TeV. The physically allowed region (unitarity limit) is bounded by the outer contour. The cross hairs are the 95% C.L. one-dimensional limits.

over the previous best results.

-
- [1] J.M. Campbell and R.K. Ellis, Phys. Rev. D **60**, 113006 (1999).
 - [2] K. Hagiwara, R.D. Peccei, D. Zeppenfeld, and K. Hikasa, Nucl. Phys. **B282**, 253 (1987).
 - [3] K. Hagiwara, S. Ishihara, R. Szalapski, and D. Zeppenfeld, Phys. Rev. D **48**, 2182 (1993). They parameterize the WWZ couplings in terms of the $WW\gamma$ couplings: $\Delta \kappa_Z = \Delta \kappa_\gamma (1 - \tan^2 \theta_W)/2$, $\Delta g_1^Z = \Delta \kappa_\gamma / (2 \cos^2 \theta_W)$ and $\lambda_Z = \lambda_\gamma$.
 - [4] DØ Collaboration, V.M. Abazov *et al.*, Phys. Rev. Lett. **95**, 141802 (2005).
 - [5] CDF Collaboration, A. Abulencia *et al.*, Phys. Rev. Lett. **98**, 161801 (2007).

- [6] D0 Collaboration, B. Abbott *et al.*, Phys. Rev. D **60**, 072002 (1999).
- [7] Particle Data Group, W.-M. Yao *et al.*, J. Phys. G **33**, 1 (2006).
- [8] D0 Collaboration, V. Abazov *et al.*, Nucl. Instrum. Methods Phys. Res. Sect. A. **565**, 463 (2006).
- [9] The D0 coordinate system is cylindrical with the z -axis along the beamline and the polar and azimuthal angles denoted as θ and ϕ respectively. The pseudorapidity is defined as $\eta = -\ln \tan \theta/2$.
- [10] D0 Collaboration, S. Abachi *et al.*, Nucl. Instrum. Methods Phys. Res. Sect. A. **338**, 185 (1994).
- [11] V. Abazov *et al.*, Nucl. Instrum. Methods Phys. Res. Sect. A. **552**, 372 (2005).
- [12] V. Abazov *et al.*, arXiv:0706.0458, submitted to Phys. Rev. D.
- [13] T. Andeen *et al.*, FERMILAB-TM-2365-E (2006).
- [14] T. Sjostrand *et al.*, Comput. Physics Commun. **135**, 238 (2001).
- [15] R. Brun *et al.*, CERN-DD-78-2-REV, 1994 (unpublished).
- [16] U. Baur and E.L. Berger, Phys. Rev. D **41**, 1476 (1990).
- [17] G.J. Feldman and R.D. Cousins, Phys. Rev. D **57**, 3873 (1998).
- [18] K. Hagiwara, J. Woodside, and D. Zeppenfeld, Phys. Rev. D **41**, 2113 (1990).
- [19] D0 Collaboration, V.M. Abazov *et al.*, Phys. Rev. Lett. **94**, 151801 (2005).
- [20] U. Baur, hep-ph/9510265 and UB-HET-95-04 (unpublished).